

# Dissipationless Quantum Spin Current at Room Temperature

Shuichi Murakami,<sup>1\*</sup> Naoto Nagaosa,<sup>1,2,3</sup> Shou-Cheng Zhang<sup>4</sup>

<sup>1</sup>Department of Applied Physics, University of Tokyo, Hongo,  
Bunkyo-ku, Tokyo 113-8656, Japan

<sup>2</sup>CERC, AIST Tsukuba Central 4, Tsukuba 305-8562, Japan

<sup>3</sup>CREST, Japan Science and Technology Corporation (JST)

<sup>4</sup>Department of Physics, McCullough Building, Stanford University,  
Stanford CA 94305-4045, USA

\*To whom correspondence should be addressed; E-mail: murakami@appi.t.u-tokyo.ac.jp.

While microscopic laws of physics are invariant under the reversal of the arrow of time, the transport of energy and information in most devices is an irreversible process. It is this irreversibility that leads to intrinsic dissipations in electronic devices and limits the possibility of quantum computation. We theoretically predict that the electric field can induce a substantial amount of dissipationless quantum spin current at room temperature, in hole doped semiconductors such as Si, Ge and GaAs. Based on a generalization of the quantum Hall effect, the predicted effect leads to efficient spin injection without the need for metallic ferromagnets. Principles found in this work could enable quantum spintronic devices with integrated information processing and storage units, operating with low power consumption and performing reversible quantum computation.

Our work is driven by the confluence of the important technological goals of quantum spintronics (1, 2) with the quest of generalizing the quantum Hall effect (QHE) to higher dimensions. The QHE is a manifestation of quantum mechanics observable at macroscopic scales. In contrast to the most transport coefficients in solid state systems, which are determined by the elastic and the inelastic scattering rates, the Hall conductance  $\sigma_H$  in QHE is quantized and completely independent of any scattering rates in the system, where the transport equation is given by  $j_\alpha = \sigma_H \epsilon_{\alpha\beta} E_\beta$  ( $j_\alpha$  and  $E_\beta$  ( $\alpha, \beta = 1, 2$ ) are the charge current and the electric fields respectively,  $\epsilon_{\alpha\beta}$  is the fully antisymmetric tensor in two dimensions). While dissipative transport coefficients are expressed in terms of states in the vicinity of the Fermi level, the non-dissipative quantum Hall conductance is expressed in terms of equilibrium response of all states below the Fermi level. The topological origin of the QHE is revealed through the fact that the Hall conductance can also be expressed as the first Chern number of a  $U(1)$  gauge connection defined in momentum space (3). Recently, the QHE has been generalized to four spatial dimensions (4). In that case, an electric field  $E_\nu$  induces an  $SU(2)$  spin current  $j_\mu^i$  ( $\mu, \nu = 1, 2, 3, 4$ ,  $i = 1, 2, 3$ ) through the non-dissipative transport equation  $j_\mu^i = \sigma \eta_{\mu\nu}^i E_\nu$ , where  $\eta_{\mu\nu}^i$  is the t'Hooft tensor, explicitly given by  $\eta_{\mu\nu}^i = \epsilon_{i\mu\nu 4} + \delta_{i\mu} \delta_{4\nu} - \delta_{i\nu} \delta_{4\mu}$  and  $\sigma$  is a dissipationless transport coefficient. The quantum Hall response in that system is physically realized through the spin-orbit coupling in a *time-reversal symmetric system*. At the boundary of this four dimensional quantum liquid, when both the electric field and the spin current are restricted to the three dimensional sub-space, the dissipationless response is given by

$$j_j^i = \sigma_s \epsilon^{ijk} E_k \quad (1)$$

This fundamental response equation shows that it is possible to induce a purely topological and dissipationless spin current by an electric field in the physical, three dimensional space.

We consider a realization of this electric field induced topological spin current in conventional hole-doped semiconductors. In a large class of semiconductors, including Si,

Ge, GaAs and InSb, the valence bands are four-fold degenerate at the  $\Gamma$ -point (see e.g. Fig. 1). The effective Luttinger Hamiltonian (5) for holes is given by

$$H_0 = \frac{\hbar^2}{2m} \left( (\gamma_1 + \frac{5}{2}\gamma_2)k^2 - 2\gamma_2(\mathbf{k} \cdot \mathbf{S})^2 \right), \quad (2)$$

where  $S_i$  is the spin-3/2 matrix. We take the hole picture, and reverse the sign of the energy. Good quantum numbers for this Hamiltonian are the helicity  $\lambda = \hbar^{-1}\mathbf{k} \cdot \mathbf{S}/k$ , and the total angular momentum  $\mathbf{J} = \hbar\mathbf{x} \times \mathbf{k} + \mathbf{S}$ . This kinetic Hamiltonian is diagonalized in the basis where the helicity operator  $\lambda$  is diagonal, and the eigenvalue is given by  $\epsilon_\lambda(\mathbf{k}) = \frac{\hbar^2 k^2}{2m} (\gamma_1 + (\frac{5}{2} - 2\lambda^2)\gamma_2) \equiv \frac{\hbar^2 k^2}{2m_\lambda}$ . For a given wave vector  $\mathbf{k}$ , the Hamiltonian (2) has two eigenvalues,  $\epsilon_H(\mathbf{k}) = \epsilon_{\lambda=\pm 3/2}(\mathbf{k}) = \frac{\gamma_1 - 2\gamma_2}{2m} \hbar^2 k^2 \equiv \frac{\hbar^2 k^2}{2m_H}$  and  $\epsilon_L(\mathbf{k}) = \epsilon_{\lambda=\pm 1/2}(\mathbf{k}) = \frac{\gamma_1 + 2\gamma_2}{2m} \hbar^2 k^2 \equiv \frac{\hbar^2 k^2}{2m_L}$ , forming Kramers doublets. They are referred to as the light-hole (LH) and heavy-hole (HH) bands. In semiconductors with zincblende structure, such as GaAs, inversion symmetry breaking causes an additional tiny splitting in the LH and HH bands. We can neglect it when the temperature is much higher than this splitting. The band structure of semiconductors deviates from the spherical to the cubic symmetry. We also neglect this effect for simplicity, because physics described below are not so much affected by it.

We shall consider the effect of a uniform electric field  $\mathbf{E}$ . Our full Hamiltonian is thus given by  $H = H_0 + V(\mathbf{x})$ , where  $V(\mathbf{x}) = e\mathbf{E} \cdot \mathbf{x}$ , and  $-e$  is the charge of an electron. We assume that the split-off band is totally occupied. We first define a  $4 \times 4$  unitary matrix  $U(\mathbf{k})$  which diagonalizes the kinetic Hamiltonian  $H_0$ .  $U(\mathbf{k})$  is defined by  $U(\mathbf{k})(\mathbf{k} \cdot \mathbf{S})U^\dagger(\mathbf{k}) = kS_z$ . In the spherical coordinates where  $\mathbf{k} = k(\sin\theta \cos\phi, \sin\theta \sin\phi, \cos\theta)$ ,  $U(\mathbf{k})$  can be expressed as  $U(\mathbf{k}) = \exp(i\theta S_y) \exp(i\phi S_z)$ . Under this unitary transformation, the new Hamiltonian  $\tilde{H} \equiv U(\mathbf{k})H U^\dagger(\mathbf{k})$  becomes

$$\tilde{H} = \frac{\hbar^2 k^2}{2m} \left( \gamma_1 + \frac{5}{2}\gamma_2 - 2\gamma_2 S_z^2 \right) + U(\mathbf{k})V(\mathbf{x})U^\dagger(\mathbf{k}) \quad (3)$$

Eigenvalues of  $S_z$  physically describe the helicity  $\lambda = \hbar^{-1}\mathbf{k} \cdot \mathbf{S}/k$  in the original basis. The kinetic part  $H_0$  now becomes diagonal, in the representation where  $S_z$  is diagonal. Because  $\mathbf{x} = i\partial_{\mathbf{k}}$ , the potential term becomes  $V(\tilde{\mathbf{D}})$ , where the covariant derivative  $\tilde{\mathbf{D}}$  is defined by  $\tilde{\mathbf{D}} = i\partial_{\mathbf{k}} - \tilde{\mathbf{A}}$  and  $\tilde{\mathbf{A}} = -iU(\mathbf{k})\partial_{\mathbf{k}}U^\dagger(\mathbf{k})$ . As  $\tilde{\mathbf{A}}$  is a pure gauge potential, there is no curvature associated with it. Up to this point, the transformation is exact. We now consider adiabatic transport and make a corresponding approximation. As is usually assumed in the transport theory, we neglect the interband transitions, i.e. the off-block-diagonal matrix elements of  $\tilde{\mathbf{A}}$  connecting the LH and HH bands. Then we arrive at a non-trivial adiabatic gauge connection  $\mathbf{A}$  (online supporting text), which takes a block-diagonal form in the LH and HH subspace. As each band is two-fold degenerate, the gauge connection is in general non-Abelian. However,  $\mathbf{A}$  has no matrix elements connecting the  $\lambda = 3/2$  and  $\lambda = -3/2$  states in the HH band, because the gauge field  $\tilde{\mathbf{A}}$  only connects

states with helicity difference  $\Delta\lambda = 0, \pm 1$ . Therefore, the non-Abelian structure is only present in the LH band. For simplicity of presentation, we shall first make an additional, *Abelian approximation* (AA), in which only the diagonal components in  $\mathbf{A}$  are retained. Afterwards, we shall give our final results including fully the non-Abelian corrections.

Within the AA,  $\mathbf{A}$  is a diagonal  $4 \times 4$  matrix in the helicity basis. As a band-touching point acts as a Dirac magnetic monopole in momentum space (6), each diagonal component of  $\mathbf{A}(\mathbf{k})$  is given by that of a Dirac monopole at  $\mathbf{k} = 0$ , with the monopole strength *eg* given by  $\lambda$ . The associated field strength is given by

$$F_{ij} \equiv i[D_i, D_j] = \epsilon_{ijk} \lambda \frac{k_k}{k^3} \quad (4)$$

The effective Hamiltonian takes the form

$$H^{\text{eff}} = \frac{\hbar^2 k^2}{2m_\lambda} + V(\mathbf{x}). \quad (5)$$

Henceforth,  $x_i$  denotes a covariant derivative in momentum space:  $x_i = D_i = i\partial/\partial k_i - A_i(\mathbf{k})$ . Note that the definition of  $x_i$  has changed by projecting the original Hamiltonian  $H$  onto the HH or LH band. While  $H^{\text{eff}}$  seems to be trivial, its non-trivial dynamics is revealed through the non-trivial commutation relations

$$[k_i, k_j] = 0, \quad [x_i, k_j] = i\delta_{ij}, \quad [x_i, x_j] = -iF_{ij}. \quad (6)$$

Such situation also happens in the Gutzwiller projection of the SO(5) model (7). It also resembles the non-trivial commutation relation between the position operators of a two-dimensional-electron-gas projected onto the lowest-Landau-level (8), where  $F_{ij} = B\epsilon_{ij}$ , and  $B$  is the external magnetic field. This general algebraic structure, called “non-commutative geometry”, also underlies the four-dimensional QHE model (4). In our present context, the non-commutativity between the three-dimensional coordinates arises from the magnetic monopole in momentum space, and it is a natural generalization of the QHE to three dimensions.

The equation of motion for holes can be derived easily from Eqs. 5 and 6 as

$$\hbar \dot{k}_i = eE_i, \quad \dot{x}_i = \frac{\hbar k_i}{m_\lambda} + F_{ij} \dot{k}_j. \quad (7)$$

The last term, proportional to  $F_{ij}$ , is a topological term, describing the effect of the magnetic monopole on the orbital motion. It represents a “Lorentz force” in momentum space, making the hole velocity non-collinear with its momentum, in contrast to the usual situations. In fact, if we interchange the roles of  $x$  and  $k$  in this term, it becomes the Lorentz force for a charged particle moving in the presence of a magnetic monopole in real space. This set of equations can be integrated analytically (supporting online text), and the resulting trajectory is shown in Fig. 2. The hole motion in real space obtains a shift

perpendicular to  $\mathbf{S}$ . This shift is analogous to the deflection of a charged particle by a magnetic monopole, in a direction perpendicular to the plane spanned by its position and velocity vectors (9). It causes a spin current perpendicular to both  $\mathbf{E}$  and  $\mathbf{S}$ . For example, for  $\mathbf{E}$  parallel to the  $+z$  direction, the spin current for each band at zero temperature, with spin parallel to the  $x$  axis, flowing to the  $y$  direction is given by

$$j_y^x = \frac{eE_z}{36\pi^2}(9k_F^H + k_F^L), \quad (8)$$

which is obtained by summing contributions from all the filled states. Here we assumed that the equilibrium momentum distribution is attained by the random impurity scattering which causes the charge relaxation. Note that Eq. 7 describes only the ballistic motion and scattering by random impurities would lead to additional contributions to the spin current. As one can see from the detailed discussions in the supporting online text, these extrinsic effects are not only small, but also scale with a higher power of  $k_F \sim n^{1/3}$ , where  $n$  is the hole density. Therefore, by plotting  $\sigma_s/n^{1/3}$  against  $n$ , and extrapolating to the limit of  $n \rightarrow 0$ , the constant intercept would uniquely determine our predicted dissipationless spin conductivity.

It is worth noting that this AA becomes exact in zero-gap semiconductors, e.g.  $\alpha$ -Sn. In this class of materials, the bottom of the conduction band and the top of the valence band correspond to the LH and HH bands in other semiconductors like GaAs. These two bands touch at  $\mathbf{k} = 0$ . In this case, p-doping introduces holes only into the HH band, and the AA becomes exact.

The electric-field-induced spin current can also be understood in terms of the conservation of the *total* angular momentum  $\mathbf{J} = \hbar\mathbf{x} \times \mathbf{k} + \mathbf{S}$ . As remarked earlier,  $\mathbf{J}$  commutes with  $H_0$ . When  $\mathbf{E}$  is parallel to the  $z$ -direction,  $J_z$  also commutes with the potential. Therefore, substituting  $\mathbf{S} = \lambda\hbar\hat{\mathbf{k}} = \lambda\hbar\mathbf{k}/k$ , we obtain

$$\dot{J}_z = \hbar(\dot{\mathbf{x}} \times \mathbf{k})_z + \hbar(\mathbf{x} \times \dot{\mathbf{k}})_z + \lambda\hbar\dot{\hat{\mathbf{k}}}_z = 0 \quad (9)$$

The second term, representing the torque, vanishes in our case since  $\dot{\mathbf{k}}$  points along the  $z$  direction. The first term  $\hbar(\dot{\mathbf{x}} \times \mathbf{k})_z$  vanishes in usual problems; however, it does not in our case, due to the non-collinearity of the velocity and the momentum. Furthermore, the first term, describing the time derivative of the orbital angular momentum  $\mathbf{L} = \hbar\mathbf{x} \times \mathbf{k}$ , is proportional to the spin current. The third term  $\lambda\hbar\dot{\hat{\mathbf{k}}}_z$  describing the time derivative of the spin angular momentum  $\mathbf{S}$ , can be easily evaluated from the acceleration equation in Eq. 7. Therefore, we see that the conservation of the total angular momentum Eq. 9 directly implies the spin current Eq. 8. The spin current flows in such a way that the change of  $\mathbf{L}$  exactly cancels the change of  $\mathbf{S}$ .

We now discuss the correction due to the non-Abelian nature of the gauge connection of the LH band. Remarkably, even though the gauge connection is non-Abelian, the associated field strength is Abelian, and gives a correction factor of  $(-3)$ , compared

to the AA (10, 11, 12). The equation of motion modified accordingly agrees with that obtained by generalizing the wave packet formalism (13) to the non-Abelian case. This non-Abelian correction gives the following result for the spin current:

$$j_y^x = \frac{eE_z}{12\pi^2}(3k_F^H - k_F^L) = \frac{\hbar}{2e}\sigma_s E_z. \quad (10)$$

Here we defined  $\sigma_s$  to have the same dimension as the electrical conductivity, to facilitate comparison. The spin current equation is rotationally invariant, with the covariant form given in Eq. 1, and is the central result of our paper. In contrast with similar effects (14, 15), this spin current has a topological character; the spin conductivity  $\sigma_s$  in Eq. 1 is independent of the mean free path and relaxational rates, and all states below the Fermi energy contribute to the spin current, where each contribution is purely determined by the gauge curvature in momentum space, similar to the QHE (3). Assuming the hole density  $n = 10^{19}\text{cm}^{-3}$ , the mobility of the holes at room temperature in GaAs is  $\mu = 50\text{cm}^2/\text{Vsec}$  (16), and the conductivity is  $\sigma = en\mu = 80\Omega^{-1}\text{cm}^{-1}$ . On the other hand, the spin Hall conductivity  $\sigma_s$  in Eq. 10 is estimated as  $\sigma_s \sim 80\Omega^{-1}\text{cm}^{-1}$ , being of the same order with  $\sigma$ . For lower carrier concentration,  $\sigma_s$  becomes larger than  $\sigma$ ; for  $n = 10^{16}\text{cm}^{-3}$ , we have  $\sigma = 0.6\Omega^{-1}\text{cm}^{-1}$  and  $\sigma_s = 7\Omega^{-1}\text{cm}^{-1}$ . At finite temperature, Eq. 10 is modified only through the Fermi distribution function  $n^\lambda(\mathbf{k})$ . Since the typical energy difference between the LH and HH bands at the same wavenumber is about 0.1eV, which largely exceeds the energy scale of the room temperature  $\sim 0.025\text{eV}$ , our predicted effect remains of the same order even at room temperature.

We remark that the non-dissipative spin transport equation Eq. 1 does not violate the time-reversal symmetry  $\mathcal{T}$ . Our microscopic Hamiltonian  $H$ , the electric field  $\mathbf{E}$  and the spin current are all  $\mathcal{T}$  invariant. Therefore, the electric field and the spin current can be related by a  $\mathcal{T}$  symmetric, dissipationless transport coefficient  $\sigma_s$ . This situation is to be contrasted with the Ohm's law. As the charge current is odd under  $\mathcal{T}$ , while the electric field is even, they can only be related by a  $\mathcal{T}$  antisymmetric, dissipative transport coefficient, namely the charge conductivity. One of the main objective in quantum computing is to achieve *reversible computation* (17, 18). From the above analysis, we see that there is a fundamental difference between the ordinary irreversible electronics computation based on the Ohm's law, and the reversible spintronics computation based on Eq. 1. The time reversal symmetry property encoded in Eq. 1 could provide a fundamental principle for the reversible quantum computation.

This spin current is also useful for spin injection into semiconductors. While effective spin injection is necessary for spintronic devices, it has been an elusive issue (2). Usage of ferromagnetic metals is not practical because most of the spin polarizations are lost at the interface due to conductivity mismatch between metal and semiconductor (19, 20). Spin injection from ferromagnetic semiconductors such as  $\text{Ga}_{1-x}\text{Mn}_x\text{As}$  has been successful (21, 22, 23). Nevertheless,  $T_c$  is at most 110K for  $\text{Ga}_{1-x}\text{Mn}_x\text{As}$ , still too low for practical use at room temperature. Thus it is desirable to find an effective method for spin injection. The

electric-field-induced spin current serves as a spin injector, because it creates a spin current *inside the semiconductor*. One might worry that the short relaxation time  $\tau_s \sim 100\text{fsec}$  (24) of the hole spins. This shortness of  $\tau_s$  is because the strong spin-orbit interaction in the valence band combines the relaxation of momenta and spins (25). Actually most of the efforts on the spintronics in GaAs have been focused on electrons in the conduction bands, having much longer spin-relaxation time ( $\sim 100\text{psec}$ ) (26). Nevertheless, our spin current is free from such rapid relaxation of spins of holes, because it is a purely quantum mechanical effect with equilibrium spin/momentum distribution. Only when the spin/momentum distribution deviates from equilibrium, e.g., in spin accumulation at boundaries of the sample, the rapid relaxation of hole spins becomes effective.

One can consider following experimental setups for detection of the constant spin supply from p-GaAs. When the electric field is applied along the  $z$ -direction and the electric current  $J_z$  is induced, the  $s^x$ -spin current  $j_y^x$  will flow along the  $y$  direction. One possibility is to see the spin-dependent electric transport through a ferromagnetic electrode with the magnetization  $\mathbf{M}$  along  $\pm x$ -direction attached to the positive- $y$  side of the sample. With a lead connecting this electrode and the other (negative- $y$ ) side of p-GaAs as shown in Fig. 3A, one should see a change of the electric current  $I$  depending on the direction of  $\mathbf{M}$ . The ratio of  $I$  when  $\mathbf{M}$  is along  $\pm x$ -direction,  $I(+x)/I(-x)$ , is expected to be well larger than unity. For the ferromagnetic electrode, ferromagnetic metals are not efficient, because of the conductance mismatch (20). Instead, ferromagnetic semiconductors will be suitable. Another possibility is to measure circular polarization of light emitted via recombination with electrons. This can be achieved by a similar experimental setup in Ref. (21), replacing (Ga,Mn)As by p-GaAs, where the quantum well structure of (In,Ga)As is sandwiched by p-GaAs and n-GaAs (Fig. 3B). The spin current injected along the  $y$ -direction will be recombined with the electrons supplied from the n-GaAs in the (In,Ga)As quantum well.

When the system is not connected to the leads along the  $y$ -direction, spins accumulate near the edges of the sample. This spin polarization can in principle be measured by the Kerr rotation. The spin distribution is determined by a balance between the spin current supply and the spin relaxation. At room temperature, because  $\tau_s = 100\text{fsec}$  (24) is rather short, the area density of spin accumulation at the sample surface,  $j_y^x \tau_s$ , is too small to be observed. However, there are several ways to make  $\tau_s$  longer. One is to lower the temperature. Another is to inject the spin into n-GaAs through the p-n junction as demonstrated recently (27, 28). The spin lifetime of electrons in GaAs is  $100\text{psec}$ ,  $10^3$  times longer than that of holes. Thereby the spin current can be detected by the Kerr rotation through surface reflection.

## References and Notes

1. G. A. Prinz, *Science* **282**, 1660 (1998).
2. S. A. Wolf *et al.*, *Science* **294**, 1488 (2001).
3. D. J. Thouless, M. Kohmoto, M. P. Nightingale, M. den Nijs, *Phys. Rev. Lett.* **49**, 405 (1982).
4. S. -C. Zhang and J. -P. Hu, *Science* **294**, 823 (2001).
5. J. M. Luttinger, *Phys. Rev.* **102**, 1030 (1956).
6. M. V. Berry, *Proc. R. Soc. Lond. A* **392**, 45 (1984).
7. S. -C. Zhang, J. -P. Hu, E. Arrigoni, W. Hanke, A. Auerbach, *Physical Review B* **60**, 13070 (1999).
8. P. Prange, S. M. Girvin, *The Quantum Hall Effect*, (Springer, Berlin, 1997).
9. J. D. Jackson, *Classical Electrodynamics* (Wiley, New York, 1998).
10. A. Zee, *Phys. Rev. A* **38**, 1 (1988). Note that there is a misprint in this reference; in the left column of page 2, the field strength should be  $F = imd\Omega$ .
11. D. P. Arovas, Y. Lyanda-Geller, *Phys. Rev. B* **57**, 12302 (1998).
12. T. Jungwirth, Q. Niu, A. H. MacDonald, *Phys. Rev. Lett.* **88**, 207208 (2002).
13. G. Sundaram, Q. Niu, *Phys. Rev. B* **59**, 14915 (1999).
14. J. E. Hirsch, *Phys. Rev. Lett.* **83**, 1834 (1999).
15. E. N. Bulgakov, K. N. Pichugin, A. F. Sadreev, P. Středa, P. Šeba, *Phys. Rev. Lett.* **83**, 376 (1999).
16. *Landolt-Börnstein: Numerical Data and Functional Relationships in Science and Technology – New Series, Group III, Volume 17, Subvolume a*, edited by O. Madelung (Springer, Berlin, 1982).
17. R. P. Feynman, A. J. G. Hey, R. W. Allen, *Feynman Lectures on Computation* (Westview Press, Boulder, 2000).
18. D. Loss and D. P. DiVincenzo, *Phys. Rev. A* **57**, 120 (1998).
19. P. R. Hammar, B. R. Bennett, M. J. Yang, Mark Johnson, *Phys. Rev. Lett.* **83**, 203 (1999).



20. G. Schmidt, D. Ferrand, L. W. Molenkamp, A. T. Filip, B. J. van Wees, *Phys. Rev. B* **62**, R4790 (2000).
21. Y. Ohno *et al.*, *Nature* **402**, 790 (1999).
22. R. Fiederling *et al.*, *Nature* **402**, 787 (1999).
23. R. Mattana *et al.*, *Phys. Rev. Lett.* **90**, 166601 (2003).
24. D. J. Hilton, C. L. Tang, *Phys. Rev. Lett.* **89**, 146601 (2002).
25. F. Meier, B.P. Zakharchenya *Optical Orientation* (North Holland, Amsterdam, 1984).
26. Y. Ohno, R. Terauchi, T. Adachi, F. Matsukura, H. Ohno, *Phys. Rev. Lett.* **83**, 4196 (1999).
27. E. Johnston-Halperin *et al.*, *Phys. Rev. B* **65**, 041306 (2002).
28. M. Kohda, Y. Ohno, K. Takamura, F. Matsukura, H. Ohno, *J. Superconductivity* **16**, 167 (2003).
29. We thank C. Herring and M. Gonokami for helpful discussions. This work is supported by Grant-in-Aids from the Ministry of Education, Culture, Sports, Science and Technology of Japan, the NSF under grant numbers DMR-9814289, and the US Department of Energy, Office of Basic Energy Sciences under contract DE-AC03-76SF00515.

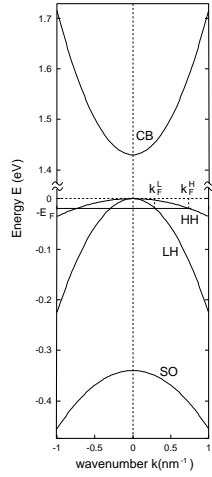


Figure 1: Approximate band structure of GaAs. We neglect the small splitting due to inversion symmetry breaking. We also neglect the anisotropy of the bands. The conduction band (CB) is two-fold degenerate. The valence band consists of the heavy hole (HH), the light hole (LH), and the split-off (SO) bands, each of which is two-fold degenerate. We consider the p-GaAs, and the Fermi momentum for each band is labelled as  $k_F^H$  and  $k_F^L$  respectively. The Fermi energy shown in the figure corresponds to  $n = 10^{19} \text{cm}^{-3}$ .

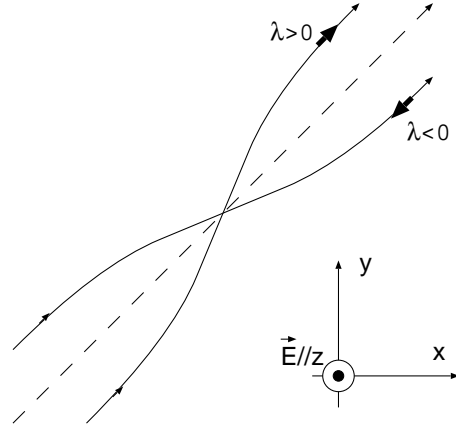


Figure 2: The real-space trajectory of the hole obtained by solving Eq.(7), The electric field  $\mathbf{E} = e^{-1}\nabla V$  is parallel to the  $+z$  direction. Due to the non-commutative relation between the components of the position operator  $x_i$ , i.e.,  $[x_i, x_j] = -iF_{ij}$  with  $F_{ij}$  being the gauge curvature defined in the momentum space, the hole obtains a transverse velocity whose direction depends on the helicity  $\lambda = \mathbf{k} \cdot \mathbf{S}/k$  indicated by the thick arrow. The broken line is parallel to  $\mathbf{k}$ .

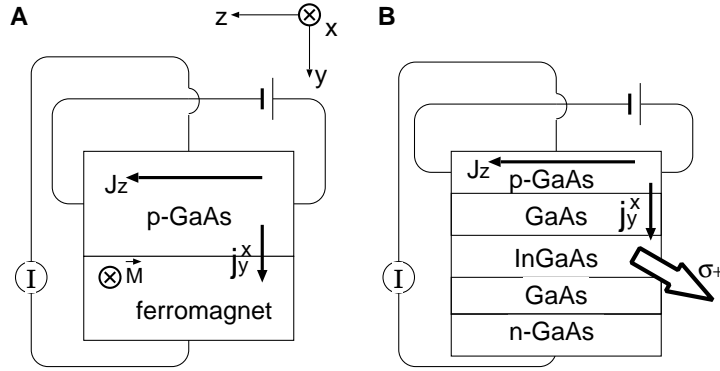


Figure 3: Experimental setups for the detection of spin current induced by an electric field. **(A)** Detection by attaching a ferromagnetic electrode. The dependence of current  $I$  flowing into the electrode on the direction of the magnetization  $\mathbf{M}$  is to be measured. **(B)** Detection by measuring the polarization of the emitted light in the quantum well of (In,Ga)As. Right and left circular polarization will be switched when the direction of the external electric field is reversed.

# Supporting online material for the article “Dissipationless Quantum Spin Current at Room Temperature”

## Luttinger Hamiltonian for semiconductors

Here we briefly summarize basic aspects of the Luttinger Hamiltonian for semiconductors. In isolated atoms, spin-orbit coupling leads to a splitting of the p orbitals into four-fold degenerate  $P_{3/2}$  and two-fold degenerate  $P_{1/2}$  levels. In a large class of semiconductors, including Si, Ge, GaAs and InSb, the  $P_{3/2}$  levels form the top of the valence bands, which are separated from  $S$ -like conduction bands. Therefore, the valence bands are four-fold degenerate and the conduction bands are two-fold degenerate at the  $\Gamma$ -point (see e.g. Fig. 1). The form of the effective Hamiltonian including spin-orbit coupling can be determined from symmetry arguments alone. In crystals with inversion symmetry, band energies depend quadratically on the momentum away from the center; therefore, a rotationally invariant Hamiltonian can only contain two possible terms,  $\mathbf{k}^2$  and  $(\mathbf{k} \cdot \mathbf{S})^2$ , where  $\mathbf{S}$  is the  $2 \times 2$  Pauli matrix for the two-fold conduction band and the  $4 \times 4$  spin matrix for the four-fold valence band. As a square of each Pauli matrix is the identity matrix, to the lowest order, there is no spin-orbit coupling in the conduction band with inversion symmetry. In the presence of inversion symmetry breaking, either due to intrinsic crystal symmetry or in hetero-junction systems, the Dresselhaus and the Rashba terms for spin-orbit coupling are possible ( $S1$ – $S3$ ). On the other hand, in the four-fold valence band, spin-orbit coupling affects the band structure, even without inversion symmetry. As the square of each component  $S_i$  ( $i = 1, 2, 3$ ) for  $S = 3/2$  is non-trivial, these two terms combine to form the effective Luttinger Hamiltonian ( $S4$ ) for holes:

$$H_0 = \frac{\hbar^2}{2m} \left( (\gamma_1 + \frac{5}{2}\gamma_2)k^2 - 2\gamma_2(\mathbf{k} \cdot \mathbf{S})^2 \right), \quad (S1)$$

where we take the hole picture, and reverse the sign of the energy. The eigenvalues are classified by the helicity  $\lambda = \hbar^{-1}\mathbf{k} \cdot \mathbf{S}/k$ ;  $\lambda = \pm 1/2$  corresponds to the LH band, and  $\lambda = \pm 3/2$  to the HH band.

## Details for calculation of $\mathbf{A}(\mathbf{k})$

The spin-3/2 matrices  $S_i$  are written as

$$S_x = \begin{pmatrix} & \frac{\sqrt{3}}{2} & & \\ \frac{\sqrt{3}}{2} & & 1 & \\ & 1 & & \frac{\sqrt{3}}{2} \\ & & \frac{\sqrt{3}}{2} & \end{pmatrix}, S_y = \begin{pmatrix} & -\frac{\sqrt{3}}{2}i & & \\ \frac{\sqrt{3}}{2}i & & -i & \\ & i & & -\frac{\sqrt{3}}{2}i \\ & & \frac{\sqrt{3}}{2}i & \end{pmatrix}, S_z = \begin{pmatrix} \frac{3}{2} & & & \\ & \frac{1}{2} & & \\ & & -\frac{1}{2} & \\ & & & -\frac{3}{2} \end{pmatrix}. \quad (S2)$$

By using  $U(\mathbf{k}) = \exp(i\theta S_y) \exp(i\phi S_z)$ , the gauge field  $\tilde{\mathbf{A}} = -iU(\mathbf{k})\partial_{\mathbf{k}}U^\dagger(\mathbf{k})$  is calculated as

$$\tilde{\mathbf{A}} \cdot d\mathbf{k} = \begin{pmatrix} -\frac{3}{2} \cos \theta d\varphi & \frac{\sqrt{3}}{2}(\sin \theta d\varphi + id\theta) & & \\ \frac{\sqrt{3}}{2}(\sin \theta d\varphi - id\theta) & -\frac{1}{2} \cos \theta d\varphi & \sin \theta d\varphi + id\theta & \\ & \sin \theta d\varphi - id\theta & \frac{1}{2} \cos \theta d\varphi & \frac{\sqrt{3}}{2}(\sin \theta d\varphi + id\theta) \\ & & \frac{\sqrt{3}}{2}(\sin \theta d\varphi - id\theta) & \frac{3}{2} \cos \theta d\varphi \end{pmatrix}, \quad (\text{S3})$$

where the first and fourth columns correspond to the HH, while the second and third ones correspond to the LH. As  $\tilde{\mathbf{A}}$  is a pure gauge potential, its curvature  $F_{ij} = i[D_i, D_j]$  vanishes. In considering adiabatic transport, we neglect the interband transitions, i.e. the off-block-diagonal matrix elements of  $\tilde{\mathbf{A}}$  between the LH and HH bands. Then we arrive at a non-trivial adiabatic gauge connection

$$\mathbf{A}' \cdot d\mathbf{k} = \begin{pmatrix} -\frac{3}{2} \cos \theta d\varphi & & & \\ & -\frac{1}{2} \cos \theta d\varphi & \sin \theta d\varphi + id\theta & \\ & \sin \theta d\varphi - id\theta & \frac{1}{2} \cos \theta d\varphi & \\ & & & \frac{3}{2} \cos \theta d\varphi \end{pmatrix}, \quad (\text{S4})$$

which takes a block-diagonal form in the LH and HH subspace. As the states in each band are two-fold degenerate, the gauge connection is in general non-Abelian. However, the non-Abelian structure is only present in the LH band; namely, in the LH subspace the matrix  $\mathbf{A}'$  has off-diagonal components, while in the HH subspace  $\mathbf{A}'$  is diagonal. This is because the gauge field  $\tilde{\mathbf{A}}$  only connects states with helicity difference  $\Delta\lambda = 0, \pm 1$ , and does not connect  $\lambda = \pm 3/2$  states in the HH band. By employing the Abelian approximation (AA) we neglect the off-diagonal elements of  $\mathbf{A}'$ , and we get thereby

$$\mathbf{A}'_{\text{Abelian}} = -S_z \cos \theta \nabla \phi, \quad (\text{S5})$$

which is diagonal in the basis where  $S_z$  is diagonal (S5). As has been recognized in (S6), the degeneracy point acts as the source of the gauge field, i.e. Dirac magnetic monopole. The present form of  $\mathbf{A}'$  corresponds to a Dirac monopole at the origin of the momentum space, with the monopole strength  $eg$  given by  $S_z$ , in accordance with (S6). To return to the original basis where the helicity  $\lambda$  becomes diagonal, we make the gauge transformation

$$\mathbf{A}_{\text{Abelian}}(\mathbf{k}) = U^\dagger(\mathbf{k})\mathbf{A}'_{\text{Abelian}}(\mathbf{k})U(\mathbf{k}) + i\frac{\partial U^\dagger(\mathbf{k})}{\partial \mathbf{k}}U(\mathbf{k}) \quad (\text{S6})$$

The monopole strength is then expressed as  $eg = \lambda$ . The associated magnetic field strength is given by

$$F_{ij} \equiv i[D_i, D_j] = \epsilon_{ijk} \lambda \frac{k_k}{k^3} \quad (\text{S7})$$

We now discuss the correction due to the non-Abelian nature of the gauge connection of the LH band. Remarkably, even though the gauge connection is non-Abelian, the associated field strength is Abelian, and is given by (S5)

$$F_{ij} = \epsilon_{ijk} \lambda \left( 2\lambda^2 - \frac{7}{2} \right) \frac{k_k}{k^3}. \quad (\text{S8})$$

This has a correction factor of  $(-3)$  only in the LH compared to the AA. As the spin current depends only on the field strength in momentum space, the spin current acquires an extra factor of  $(-3)$  only in the LH, compared with that within the AA.

## Real-space trajectory of the hole motion

The equation of motion (Eq. 7) within the AA can be integrated analytically. When  $\mathbf{E}$  is parallel to the  $+z$  direction, we get

$$\begin{aligned} k_x(t) &= k_{x0}, \quad k_y(t) = k_{y0}, \quad k_z(t) = k_{z0} + eE_z t/\hbar, \\ z(t) &= z_0 + \frac{\hbar k_{z0}}{m_\lambda} t + \frac{eE_z}{2m_\lambda} t^2, \\ x(t) &= x_0 + \frac{\hbar k_{x0}}{m_\lambda} t - \frac{\lambda k_{y0}}{k_{x0}^2 + k_{y0}^2} \frac{eE_z t/\hbar + k_{z0}}{\sqrt{k_{x0}^2 + k_{y0}^2 + (eE_z t/\hbar + k_{z0})^2}}, \\ y(t) &= y_0 + \frac{\hbar k_{y0}}{m_\lambda} t + \frac{\lambda k_{x0}}{k_{x0}^2 + k_{y0}^2} \frac{eE_z t/\hbar + k_{z0}}{\sqrt{k_{x0}^2 + k_{y0}^2 + (eE_z t/\hbar + k_{z0})^2}}. \end{aligned}$$

The last terms in  $x(t)$  and  $y(t)$  represent a shift of the particle position, in a direction perpendicular to  $\mathbf{k}$ , as presented in Fig. 2. As the directions of the spin is parallel (antiparallel) to  $\mathbf{k}$  for  $\lambda > 0$  ( $\lambda < 0$ ), the hole motion in real space obtains a shift perpendicular to  $\mathbf{S}$ . This shift causes a spin current perpendicular to both  $\mathbf{E}$  and  $\mathbf{S}$ .

## Calculation of spin current

The motion along the  $z$ -direction in the equation of motion (Eq. 7) is free acceleration by the electric field. In reality, because this acceleration is suppressed by random scattering we should take into account the charge relaxation by random scattering as is discussed in details in the next section. For example, the spin current for each band at zero temperature, with spin parallel to the  $x$  axis, flowing to the  $y$  direction is given by

$$j_y^{xH} = \frac{\hbar}{3} \sum_{\lambda=\pm\frac{3}{2}, \mathbf{k}} \dot{y} \frac{\lambda k_x}{k} n^\lambda(\mathbf{k}) = \frac{3e}{2} E_z \sum_{\mathbf{k}} \frac{n^H(\mathbf{k}) k_x^2}{k^4} = \frac{eE_z k_F^H}{4\pi^2}, \quad (\text{S9})$$

$$j_y^{xL} = \frac{\hbar}{3} \sum_{\lambda=\pm\frac{1}{2}, \mathbf{k}} \dot{y} \frac{\lambda k_x}{k} n^\lambda(\mathbf{k}) = \frac{e}{6} E_z \sum_{\mathbf{k}} \frac{n^L(\mathbf{k}) k_x^2}{k^4} = \frac{eE_z k_F^L}{36\pi^2}, \quad (\text{S10})$$

where  $n^\lambda(\mathbf{k})$  is a filling of holes in the band with helicity  $\lambda$ ;  $n^{\pm 3/2}(\mathbf{k}) = n^H(\mathbf{k})$  and  $n^{\pm 1/2}(\mathbf{k}) = n^L(\mathbf{k})$  are fillings for the HH and LH bands, respectively. Charge relaxation is already included in this result by putting the Fermi surfaces as in their equilibrium position  $|\mathbf{k}| = k_F$ . We have taken into account that the expectation value of the electron spin  $\mathbf{s}$  is one-third of that of  $\mathbf{S}$ :  $\mathbf{s} = \frac{1}{3}\mathbf{S}$ . This is because the spin-3/2 matrix  $\mathbf{S}$  is a summation of the spin angular momentum  $\mathbf{s}$  with spin one-half and the atomic orbital angular momentum  $\mathbf{l}$  with spin one ( $S_4$ ).

By including the non-Abelian correction in the LH band (Eq. S8), the spin current is given by

$$\begin{aligned}
j_y^x &= \frac{\hbar}{3} \text{tr} \sum_{\mathbf{k}} \dot{y}^n(\mathbf{k}) S_x n^\lambda(\mathbf{k}) = \frac{eE_z}{3} \text{tr} \sum_{\mathbf{k}} F_{yz}(\mathbf{k}) S_x n^\lambda(\mathbf{k}) \\
&= \frac{eE_z}{3} \text{tr} \sum_{\mathbf{k}} \frac{k_x S_x}{k^3} \lambda \left( 2\lambda^2 - \frac{7}{2} \right) n^\lambda(\mathbf{k}) = \frac{eE_z}{9} \sum_{\mathbf{k}, \lambda} \frac{1}{k^2} \lambda^2 \left( 2\lambda^2 - \frac{7}{2} \right) n^\lambda(\mathbf{k}) \\
&= \frac{eE_z}{12\pi^2} (3k_F^H - k_F^L). \tag{S11}
\end{aligned}$$

Interestingly, in the Ioffe-Regel limit of  $k_F l \sim 1$  the size of the spin conductivity is comparable to that of the charge conductivity  $\sigma \sim k_F^2 l$ .

The formula, Eq. S11, is at zero temperature; for finite temperature, it is modified only through the Fermi distribution function  $n^\lambda(\mathbf{k})$ . For example, at room temperature and  $n = 10^{19} \text{cm}^{-3}$ , the nominal value of the energy difference between the LH and HH bands at the same wavenumber is 0.1eV, and it largely exceeds both the temperature ( $\sim 0.025 \text{eV}$ ) and the energy scale for momentum relaxation  $\hbar/\tau_p \sim 0.006 \text{eV}$ , where we estimated the momentum relaxation time  $\tau_p$  to be of the same order ( $S7$ ) as the spin relaxation time for holes  $\tau_s \sim 100 \text{fsec}$  ( $S8$ ). Thus the value of the spin current remains of the same order as in the zero temperature.

## Impurity scattering and relaxation

Our equation of motion Eq. 7 describes only the ballistic motion, and the relaxation process due to the random scattering by impurities and phonons are not explicitly taken into account. The relaxation is essential to attain the thermal equilibrium, which we assumed to obtain Eq. 10. Our result is similar to the Karplus-Luttinger (KL) term ( $S9$ ) in the context of the anomalous Hall effect (AHE). The effects of the random scatterings have been discussed in the context of AHE by many authors ( $S10$ – $S14$ ); here we shall use some of these results to estimate the impurity contribution to the spin current. Kohn-Luttinger ( $S11$ ) and Luttinger ( $S12$ ) derived the formula for AHE based on the rigorous treatment of the density matrix in the expansion of the impurity scattering strength  $v$ , reproducing all the contributions to  $\sigma_{xy}$  up the  $v^0$  order. The skew scattering contribution proposed by Smit ( $S10$ ) is of the order of  $v^{-1}$ , and hence is expected to be important in

the weak disorder case. However it is proportional to  $\langle V^3 \rangle_c$  ( $V$  is the impurity potential, and  $\langle \rangle_c$  is the cumulant average) and hence vanishes for the Gaussian distribution of the disorder potential. Furthermore, this skew scattering mechanism predicts  $\rho_H \propto \rho$  ( $\rho$ : Hall resistivity,  $\rho$ : diagonal resistivity), which is not usually observed experimentally including the doped GaAs. The contribution of the order of  $v^0$  contains two terms, both of which are independent of the scattering. One is the KL term, which is similar to our dissipationless spin current, and the other term is later interpreted by Berger (S13) as the side-jump contribution accompanied by the impurity scattering. In the following, we shall estimate their relative magnitudes and point out the important fact that they scale differently with the hole density  $n$ , and can therefore be uniquely distinguished in the low density limit.

In the present case of GaAs, there are several evidences that the intrinsic AHE (KL term) is the dominant contribution. Jungwirth et al. (S15) showed that KL term explains the experimentally observed  $\sigma_{xy}$  quantitatively for ferromagnetic (Ga,Mn)As and (In,Mn)As. Especially the difference between (Ga,Mn)As and (In,Mn)As is successfully attributed to the different ratio  $m_{LH}/m_{HH}$  of the effective masses of light- and heavy hole bands. Also one can estimate the contribution of side jump and skew scattering as follows. By modifying the expression for the AHE due to side jump mechanism (S13,S14), the side-jump contribution to the spin Hall conductance is given by

$$\sigma_s^{\text{side jump}} = -\frac{\alpha e^2 \lambda_c^2}{2\hbar} n \quad (\text{S12})$$

where  $\lambda_c = \hbar/mc = 3.86 \times 10^{-11} \text{cm}$  is the Compton wave length of free electron, and  $\alpha$  is the enhancement factor for the Bloch electrons which is estimated to be around  $10^4$ . In terms of this estimation one can estimate its ratio to the spin Hall conductance  $\sigma_s$  in Eq. 10 as

$$\frac{|\sigma_s^{\text{side jump}}|}{\sigma_s} \cong \alpha(\lambda_c k_F)^2 \quad (\text{S13})$$

which is around  $10^{-3}$  even for the density as high as  $n = 10^{20} \text{cm}^{-3}$ . Therefore it is expected to be negligible. As for the skew scattering contribution, it is at most of the order of

$$\frac{|\sigma_s^{\text{skew scattering}}|}{\sigma_s} \cong \alpha(\lambda_c k_F)^2 \sqrt{\frac{\varepsilon_F \tau p}{\hbar}} \quad (\text{S14})$$

which is again much smaller than unity for the reasonable value of  $\sqrt{\frac{\varepsilon_F \tau}{\hbar}} \sim 10$ . Therefore we have the good reason to expect that our  $\sigma_s$  in Eq. 10 gives the dominant contribution, and hence the spin current estimated in this paper can be observed in hole doped GaAs.

From Eqs. S12, S13 and S14, we see that the side jump and the skew scattering contributions scale with the hole density like  $n$  and  $n^{4/3}$  respectively, while our dissipationless spin conductivity  $\sigma_s$  scales like  $n^{1/3}$ . Therefore, one can plot the experimentally observed total spin conductivity as  $\sigma_s^T/n^{1/3}$  versus  $n$ , and extrapolate to the limit of  $n \rightarrow 0$ . Only



the dissipationless spin conductivity contributes to the constant intercept in this limit, and it can therefore be distinguished from the impurity effects in an unique way.

## Experimental detection of the spin current

In detecting the spin current by attaching a ferromagnetic electrode as in Fig. 3A, one should see a change of the electric current  $I$  depending on the direction of  $\mathbf{M}$ . For  $n = 10^{19} \text{cm}^{-3}$ , the spin current density  $j_y^x$  is estimated as  $2e\hbar^{-1}j_y^x = (\sigma_s/\sigma)J_z \sim J_z$ . The spin current  $j_y^x$  induces the electric current  $I$  when the magnetization of the electrode is along  $+x$ -direction; no current is observed for  $-x$ -direction, when the ferromagnetic electrode is a half-metal. In realistic situation, the ratio of the electric currents  $I(+x)/I(-x)$  is determined by that of the tunneling probabilities for parallel and anti-parallel spins at the interface with the electrode. This ratio is still expected to be well larger than unity.

Another method of experimental detection of the spin current is to measure circular polarization of light emitted via recombination with electrons as in Fig. 3B. With the steady electric current  $J_z$  within the layer, the spin current injected along the  $y$ -direction will be recombined with the electrons supplied from the n-GaAs in the (In,Ga)As quantum well. This can be regarded as the p-n junction with the opposite voltage for opposite direction of the spin  $s_x$ . Therefore the current along the circuit is different between up- and down-spins with different direction, and hence the finite current is observed for  $I$ .

One can also detect the spin current by measuring the spins accumulated near the edges of the sample. The distribution of spin accumulation is determined by a balance between the spin current supply and the spin relaxation. A diffusion equation for hole spins can be written as

$$\frac{\partial s_x(y, t)}{\partial t} - D \frac{\partial^2 s_x(y, t)}{\partial y^2} = - \frac{\partial j_y^x(y, t)}{\partial y} - \frac{s_x(y, t)}{\tau_s} \quad (\text{S15})$$

where  $D = \mu k_B T / e$  is the diffusion constant. For simplicity, let us assume a semi-infinite sample extending for  $y < 0$ . Considering a steady state and the spin current being assumed to be  $j_y^x(x) = j_y^x \theta(-y)$ , we can solve the above diffusion equation as

$$s_x(y) = j_y^x \sqrt{\frac{\tau_s}{D}} e^{\frac{y}{\sqrt{D\tau_s}}}. \quad (\text{S16})$$

This solution means that the spins are distributed within the length scale  $L = \sqrt{D\tau_s}$  with the total amount  $j_y^x \tau_s$  per unit area. At room temperature, from  $\tau_s = 100 \text{fsec}$  (S8) the length scale  $L$  is estimated as  $L \cong 4 \text{nm}$ . We estimate the upper bound for the electric current density as  $10^4 \text{A/cm}^2$ , and the corresponding spin current  $2ej_y^x \sim 10^4 \text{A/cm}^2$ . Therefore the spin density integrated over the depth is given by  $j_y^x \tau_s \sim 3 \times 10^9 \mu_B \text{cm}^{-2}$ , too small to be observed optically. However there are several ways to overcome this difficulty. One is to lower the temperature. At  $T = 30 \text{K}$ ,  $\tau_s$  reaches around  $\tau_s \sim 30 \text{psec}$  (S16), nearly 300 times larger than that of room temperature. and the total spin density

becomes  $\sim 10^{12}\mu_{\text{B}}\text{cm}^{-2}$ . Another possibility is to inject the spin into n-GaAs through the p-n junction. The spin lifetime of electrons in GaAs is 100psec,  $10^3$  times longer than that of holes, and by suppressing the D'yakonov-Perel' mechanism it could be even as long as 2nsec (S17). Therefore the accumulation depth  $L$  becomes  $(0.1-1)\mu\text{m}$ , comparable to the wavelength of the visible light, with the area density  $10^{12}-10^{13}\mu_{\text{B}}\text{cm}^{-2}$  for the spins near the edges of the n-type GaAs. Therefore it can be detected by the Kerr rotation through surface reflection.

## Supporting references and notes

- S1. G. Dresselhaus, *Physical Review* **100**, 580 (1955).
- S2. E. I. Rashba, *Soviet Physics, Solid State* **2**, 1109 (1960).
- S3. Y. A. Bychkov and E. I. Rashba. *Journal of Physics C* **17**, 6039 (1984).
- S4. J. M. Luttinger, *Phys. Rev.* **102**, 1030 (1956).
- S5. A. Zee, *Phys. Rev. A* **38**, 1 (1988). Note that there is a misprint in this reference; in the left column of page 2, the field strength should be  $F = imd\Omega$ .
- S6. M. V. Berry, *Proc. R. Soc. Lond. A* **392**, 45 (1984).
- S7. F. Meier, B.P. Zakharchenya *Optical Orientation* (North Holland, Amsterdam, 1984).
- S8. D. J. Hilton, C. L. Tang, *Phys. Rev. Lett.* **89**, 146601 (2002).
- S9. R. Karplus and J. M. Luttinger, *Physical Review* **95**, 1154 (1954).
- S10. J. Smit, *Physica* **21**, 877 (1955); *Physica* **24**, 39 (1958).
- S11. W. Kohn and J. M. Luttinger, *Physical Review* **108**, 590 (1957).
- S12. J. M. Luttinger, *Physical Review* **112**, 739 (1958).
- S13. L. Berger, *Physical Review B* **2**, 4559 (1970).
- S14. A. Crépieux and P. Bruno, *Physical Review B* **64**, 014416 (2001).
- S15. T. Jungwirth, Q. Niu, A. H. MacDonald, *Phys. Rev. Lett.* **88**, 207208 (2002).
- S16. S. Adachi, T. Miyashita, S. Takeyama, Y. Takagi, A. Tackeuchi, *J. Lumin.* **72-74**, 307 (1997).
- S17. Y. Ohno, R. Terauchi, T. Adachi, F. Matsukura, H. Ohno, *Phys. Rev. Lett.* **83**, 4196 (1999).